Postprint of: Niedźwiecki M., Pietrzak P., High-Precision FIR-Model-Based Dynamic Weighing System, IEEE Transactions on Instrumentation and Measurement, Vol. 65, Iss. 10 (2016), pp. 2349-2359, DOI: 10.1109/TIM.2016.2575180

High-precision FIR-model based dynamic weighing system

Maciej Niedźwiecki, *Senior Member, IEEE,* and Przemysław Pietrzak

***Abstract*—Conveyor belt type checkweighers are increasingly popular components of modern production lines. They are used to asses the weight of the produced items in motion, i.e., without stopping them on the weighing platform. The main challenge one faces when designing a dynamic weighing system is providing high measurement accuracy, especially at high conveyor belt speeds. The approach proposed in this paper can be characterized as a filtering scheme based on the FIR model of the weighing system response. It is shown that when such a model-based filtering is applied, the attained weighing accuracy is up to four times higher than that guaranteed by the currently available state-of-the-art solutions.**

***Index Terms*—Dynamic mass measurement, conveyor belt type checkweighers, model-based filtering.**

I. Introduction

Conveyor belt type checkweighers are increasingly popular components of modern production lines. They are used to asses the weight of the produced items in motion, i.e., without stopping them on the weighing platform. Precise weight measurement is needed to generate the product labels (including the price, if the price is weight-dependent) or to eliminate products that are defective (e.g. incomplete multipacks) or which do not comply with the desired weight specification (items that are outside the tolerance are automatically taken out of line) [1]. There are many other applications of dynamic weighing including weighing of cars [2], [3] and trains [4], [5].

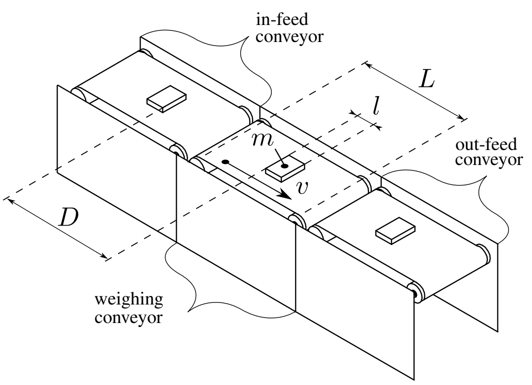

Fig. 1. A conveyor belt type checkweigher.

M. Niedźwiecki is with the Department of Electronics, Telecommunications and Informatics, Gdańsk University of Technology, Gdańsk, Poland, e-mail: maciekn@eti.pg.gda.pl.

P. Pietrzak is with the Department of Control and Measurement, West Pomeranian University of Technology, Szczecin, Poland, e-mail: pietrzak@zut.edu.pl.

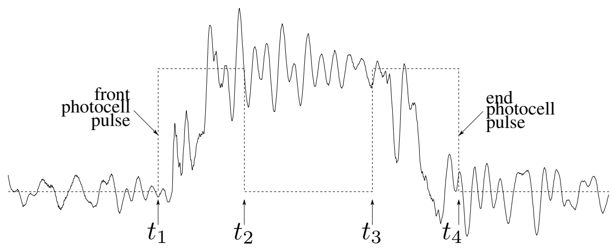

Fig. 2. Typical responses of the load cell (solid line) and front/end photocells (dotted line) observed during one weighing cycle. The signal shown in this figure was obtained for the load $m = 300\,\text{g}$ under conveyor belt speed $v = 1.2\,\frac{\text{m}}{\text{s}}$. The length $t_4 - t_1$ of the entire weighing cycle was equal to 400 ms.

An example of the conveyor belt catchweigher is schematically depicted in Fig. 1. The system is equipped with two photocells located between the in-feed conveyor and weighing conveyor, and between the weighing conveyor and the out-feed conveyor, respectively. Both photocells generate signals that allow one to precisely localize the three stages of weighing (see Fig 2): the period $[t_1, t_2]$ during which the weighed item slides onto the weighing platform, the period $(t_2, t_3]$ during which the entire item remains on the platform, and the period $(t_3, t_4]$ during which the item slides off the platform. In our study we will use the data from the first two stages.

Since the weighed items are transported with a high speed (often exceeding 1m/s), the signal obtained from the strain gauge load cell attached to the weighing platform is highly oscillatory, never reaching its steady state value corresponding to the item's static weight. Additionally, the measurements are corrupted with several kinds of disturbances, such as low frequency vibrations caused by internal and external sources (called environmental vibrations) and measurement noise [6], [7], [8]. For this reason the signal obtained from the strain gauge must be processed in a special way in order to "extract" the static weight information from the transient response of the system.

Basically, two different approaches to dynamic weighing were described in the literature. In the model-based approach the measured signal is modeled as a response of a linear dynamic IIR (infinite impulse response) system with unknown parameters to a pulse-like excitation. During each weighing cycle the model is identified based on the collected measurements. The obtained estimates of model parameters are next used to calculate the steady state response of the weighing platform to a hypothetical step-like excitation, i.e., the static weight of the weighed item [9], [2], [4], [10].

The second, model-free filtering approach to dynamic weighing incorporates digital filters designed so as to reduce the noise and attenuate the oscillatory part of the system response. The weight estimate can be obtained by reading out the signal observed at the output of the filter at the instant t_3, i.e., at the end of the second weighing stage, just before the weighed item starts to slide off the weighing platform. As shown in [11], [12], [13],[14], [15], [16] very good results can be obtained if the classical time-invariant filtering scheme is replaced with a time-varying (i.e., variable-bandwidth) one. Another model-free method, proposed in [17], is based on subspace identification and does not rely on direct data filtering. It shares some properties with the model-based approach, e.g. it does not require pre-tuning.

When optimized, the model-based and model-free time-variant filtering approaches yield comparable results [10]. In the case of the model-based approach optimization amounts to the appropriate choice of the model structure, identification technique and prefilter used to process the data prior to identification. In the case of time-variant filtering (model-free) approach, one has to optimize, for a particular system at hand, the order and coefficients of a digital filter. The filtering approach is computationally less demanding but requires off-line tuning of design parameters. The advantage of the model-based approach is that it can be operated in a fully autonomous manner (without pre-tuning) under different operating conditions.

The approach proposed in this paper can be characterized as a filtering scheme based on the FIR (finite impulse response) model of the steady state response of the weighing system. Hence, to some extent, it can be regarded as a combination of the two techniques described earlier. Similar to all model-free filtering solutions, the new approach requires off-line tuning for given operating conditions (conveyor belt speed, sampling frequency) and a given load range. However, since the model-based filtering is applied, the attained weighing accuracy is up to four times higher than that guaranteed by the existing solutions.

II. Weight estimation based on global modeling

Denote by $\mathcal{Y}^{ij}(N) = \{y^{ij}(1), \dots, y^{ij}(N)\}$ the j-th realization of the dynamic weight measurement of the load m_i for a given conveyor belt speed v and a given sampling frequency f. The measurement process starts at the moment $t = t_1 = 1$ at which the weighed item starts to slide onto the weighing section, and ends at the instant $t = t_3 = N$ at which it starts to slide off the weighing section [here and later $t = 1, 2, \dots$ denotes the normalized (dimensionless) discrete time]. To obtain training data, each load m_i, $i = 1, \dots, I$ is weighed J times. Fig. 3, which shows the superposition of $J = 240$ weighings obtained for 3 test loads $m_1 = 25$ g, $m_5 = 350$ g, $m_7 = 750$ g), 3 conveyor belt speeds ($v_1 = 0.54$ m/s, $v_2 = 0.94$ m/s, $v_3 = 1.34$ m/s) and a sampling rate $f_2 = 1600$ Hz gives some idea of the data variability and repeatability. Since it is the conveyor belt transport system, and not the load cell, that is the main source of nonvanishing measurement errors, one should not be surprised by the low signal-to-noise ratio, especially for small loads.

A. FIR model

We will assume that at a given time instant $t \in T = [1, N]$ the mass of the weighed item can be closely approximated by a linear combination of past measurements, namely

$$m_i = \boldsymbol{h}_n^{\mathrm{T}} \boldsymbol{\varphi}_n^{ij}(t) + e^{ij}(t), \quad i = 1, \dots, I, \; j = 1, \dots, J \qquad (1)$$

where

$$\boldsymbol{h}_n = [h_1, \dots, h_n]^{\mathrm{T}}$$

denotes the vector of unknown model coefficients,

$$\boldsymbol{\varphi}_n^{ij}(t) = [y^{ij}(t), \dots, y^{ij}(t - n + 1)]^{\mathrm{T}}$$

denotes the regression vector made up of $n \leq t$ past measurements, and $e^{ij}(t)$ denotes the corresponding modeling error.

Since the quantity m_i appearing on the left hand side of (1) is deterministic (as it is the true mass, rather than its measurement), equation (1) does not constitute the classical regression model, where the quantity $e^{ij}(t)$ would be regarded as the "measurement error". The term $\boldsymbol{h}_n^{\mathrm{T}} \boldsymbol{\varphi}_n^{ij}(t)$ can be interpreted as a linear approximation of m_i in terms of experimental data, i.e., a linear model of the steady state system response. In the next subsection we will optimize this model so that the fit is good in the considered range of loads and a selected range of t values.

B. Estimation of model parameters

To obtain the global model, covering the entire measurement range, we will combine all available training data: $\mathcal{D}(N) = \{\mathcal{Y}^{ij}(N), i = 1, \dots, I, \; j = 1, \dots, J\}$. Parameter estimation will be based on minimization of the following global performance measure

$$\mathcal{J}[\boldsymbol{h}_n, \mathcal{D}(N)] = \sum_{t=N-M+1}^{N} \sum_{i=1}^{I} \sum_{j=1}^{J} [m_i - \boldsymbol{h}_n^{\mathrm{T}} \boldsymbol{\varphi}_n^{ij}(t)]^2 \qquad (2)$$

which results in

$$\begin{aligned} \widehat{\boldsymbol{h}}_n(N) &= \arg\min_{\boldsymbol{h}_n} \mathcal{J}[\boldsymbol{h}_n, \mathcal{D}(N)] \\ &= \left[\sum_{t=N-M+1}^{N} \sum_{i=1}^{I} \sum_{j=1}^{J} \boldsymbol{\varphi}_n^{ij}(t) [\boldsymbol{\varphi}_n^{ij}(t)]^{\mathrm{T}} \right]^{-1} \\ &\times \left[\sum_{t=N-M+1}^{N} \sum_{i=1}^{I} \sum_{j=1}^{J} \boldsymbol{\varphi}_n^{ij}(t) m_i \right] \end{aligned} \qquad (3)$$

provided, of course, that the regression matrix in (3) is nonsingular. Note that the performance measure (2) favors models that guarantee good fit to experimental data at M locations ending the weighing period. The main purpose of adopting $M > 1$ is to make the model robust to the possible phase shifts of the scale's response. The limited repeatability of this response, evident after examining the plots shown in Fig. 3, is usually caused by slight changes in the orientation of weighed items that take place during their transportation along the conveyor belt system. According to our experiments $M = 20$ is a good choice.

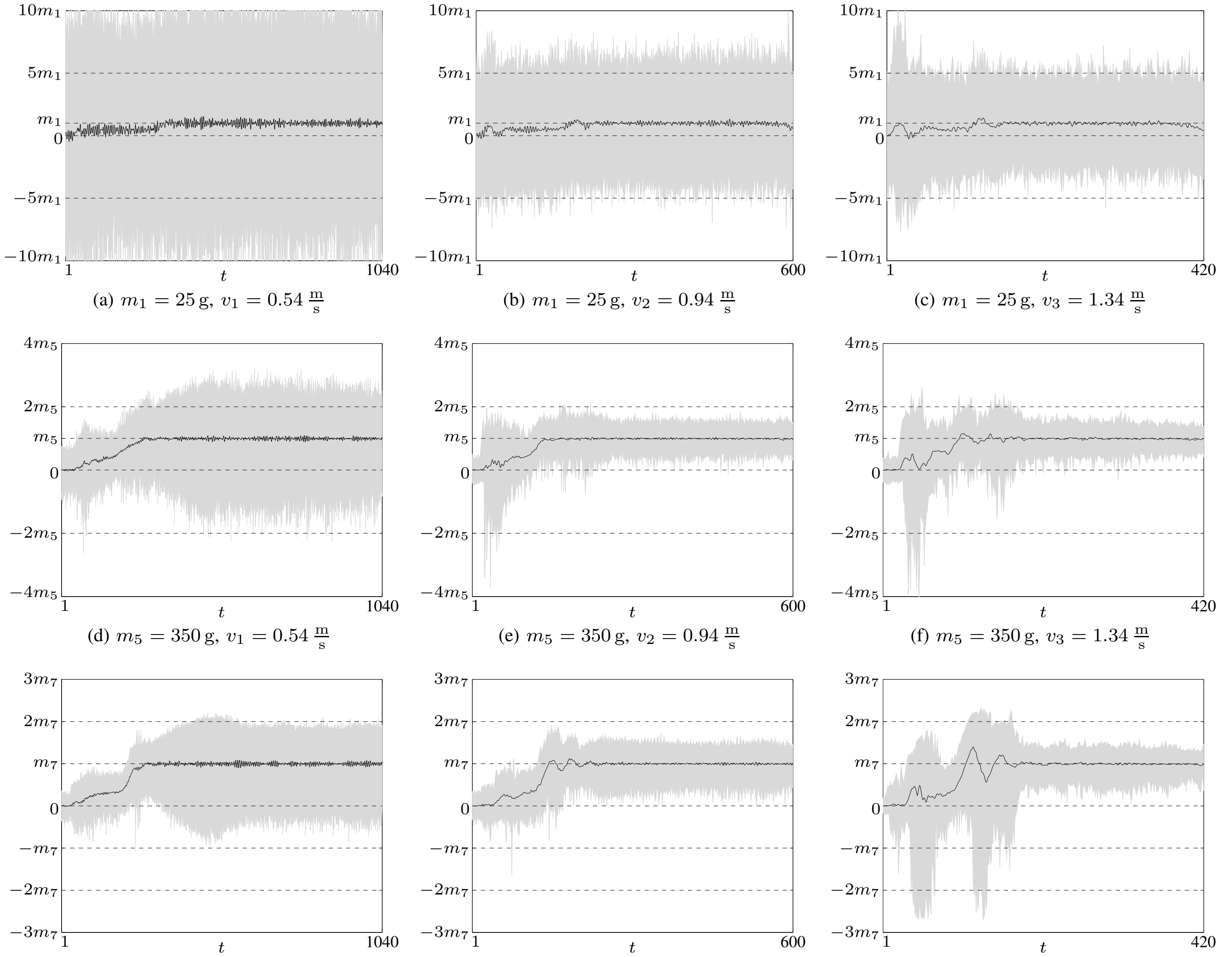

(a) $m_1 = 25\,\mathrm{g}$, $v_1 = 0.54\,\frac{\mathrm{m}}{\mathrm{s}}$ (b) $m_1 = 25\,\mathrm{g}$, $v_2 = 0.94\,\frac{\mathrm{m}}{\mathrm{s}}$ (c) $m_1 = 25\,\mathrm{g}$, $v_3 = 1.34\,\frac{\mathrm{m}}{\mathrm{s}}$

(d) $m_5 = 350\,\mathrm{g}$, $v_1 = 0.54\,\frac{\mathrm{m}}{\mathrm{s}}$ (e) $m_5 = 350\,\mathrm{g}$, $v_2 = 0.94\,\frac{\mathrm{m}}{\mathrm{s}}$ (f) $m_5 = 350\,\mathrm{g}$, $v_3 = 1.34\,\frac{\mathrm{m}}{\mathrm{s}}$

(g) $m_7 = 750\,\mathrm{g}$, $v_1 = 0.54\,\frac{\mathrm{m}}{\mathrm{s}}$ (h) $m_7 = 750\,\mathrm{g}$, $v_2 = 0.94\,\frac{\mathrm{m}}{\mathrm{s}}$ (i) $m_7 = 750\,\mathrm{g}$, $v_3 = 1.34\,\frac{\mathrm{m}}{\mathrm{s}}$

Fig. 3. Superposition of the results of 240 weighings obtained for 3 test loads and 3 conveyor belt speeds under the sampling rate of 1600 Hz. Black lines show the ensemble averages: $\bar{y}^i(t) = (1/240)\sum_{j=1}^{240} y^{ij}(t),\ t = 1, \dots, N$.

C. Weight estimation

Denote by $\mathcal{S}(N) = \{s(1), \dots, s(N)\}$ the set of measurements collected during normal on-line operation of the dynamic weighing system. We will assume that the data set $\mathcal{S}(N)$ was obtained under the same operating conditions (conveyor belt speed, sampling frequency) as those used to obtain the training data $\mathcal{D}(N)$. Based on (1) and (3) the estimate of the item's weight can be obtained from

$$\widehat{m}(N) = \widehat{\boldsymbol{h}}_n^{\mathrm{T}}(N)\boldsymbol{\psi}_n(N) \tag{4}$$

where

$$\boldsymbol{\psi}_n(N) = [s(N), \dots, s(N-n+1)]^{\mathrm{T}}$$

III. Model order selection

So far we have assumed that the order n of the model (1) is known and fixed prior to parameter estimation. Preliminary experiments, involving real-world data, have shown that the choice of n can strongly influence accuracy of weight measurement. When the order is set to its maximum allowable value $N - M + 1$ (which means that all available samples are incorporated in the estimation process) the obtained results are not satisfactory. To solve the order selection problem, three methods were implemented and evaluated: the Akaike information criterion (AIC) [18], the Bayesian information criterion (BIC) [19], and the method of cross validation (CV) [20].

A. Information criteria

The Akaike information criterion is based on maximization of the penalized log likelihood function of the experimental data, leading to

$$\widehat{n}(N) = \arg \min_{n \in [1, N-M+1]} \mathrm{AIC}(n) \tag{5}$$

where

$$\mathrm{AIC}(n) = K \log \mathrm{RSS}(n) + 2n. \tag{6}$$

RSS(n) denotes the residual sum of squared modeling errors

$$\mathrm{RSS}(n) = \sum_{t=t-M+1}^{N} \sum_{i=1}^{I} \sum_{j=1}^{J} \left[m_i - \widehat{\boldsymbol{h}}_n^{\mathrm{T}}(N) \boldsymbol{\varphi}_n^{ij}(t) \right]^2 \quad (7)$$

and $K = IJM$ denotes the number of different "input-output" pairs $\{m_i, \boldsymbol{\varphi}_n^{ij}(t)\}$ incorporated in (3).

In the Bayesian version of the information criterion

$$\mathrm{BIC}(n) = K \log \mathrm{RSS}(n) + n \log K \quad (8)$$

the "penalty" for overestimation of the model order ($n \log K$) is stronger than the analogous penalty in the Akaike criterion ($2n$). For this reason model orders selected using BIC

$$\widehat{n}(N) = \arg \min_{n \in [1, N-M+1]} \mathrm{BIC}(n) \quad (9)$$

are usually lower than those selected by AIC.

B. Cross validation

Derivation of both information criteria, summarized above, is based on the assumption that the sequence of modeling errors $\{e^{ij}(t)\}$ is a realization of white Gaussian noise, which in the case considered is obviously not true, especially in the initial phase of weighing. For this reason the indications of the information criteria should be used with caution. The method of model order selection that does not rely on such an unrealistic assumption is based on the concept of cross validation. In order to use this method, the available data set $\mathcal{D}(N)$ should be divided into two subsets: the one

$$\mathcal{D}_1(N) = \{\mathcal{Y}^{ij}(N), i = 1, \ldots, I, j = 1, \ldots, J/2\}$$

that is used for the purpose of model parameter estimation only, and another one

$$\mathcal{D}_2(N) = \{\mathcal{Y}^{ij}(N), i = 1, \ldots, I, j = J/2 + 1, \ldots, J\}$$

that is used for the purpose of selection of the most appropriate model order, i.e., the number of estimated coefficients [we have assumed that J is an even number; generally, any random division of $\mathcal{D}(N)$ into $\mathcal{D}_1(N)$ and $\mathcal{D}_2(N) = \mathcal{D}(N) - \mathcal{D}_1(N)$ can be applied].

Based on $\mathcal{D}_1(N)$ the following least squares estimates can be computed

$$\begin{aligned} \widehat{\boldsymbol{h}}_n(N) &= \arg \min_{\boldsymbol{h}_n} \mathcal{J}[\boldsymbol{h}_n, \mathcal{D}_1(N)] \\ &= \left[\sum_{t=N-M+1}^{N} \sum_{i=1}^{I} \sum_{j=1}^{J/2} \boldsymbol{\varphi}_n^{ij}(t) [\boldsymbol{\varphi}_n^{ij}(t)]^{\mathrm{T}} \right]^{-1} \\ &\quad \times \left[\sum_{t=N-M+1}^{N} \sum_{i=1}^{I} \sum_{j=1}^{J/2} \boldsymbol{\varphi}_n^{ij}(t) m_i \right]. \end{aligned} \quad (10)$$

for different values of n. The obtained models are next validated using the subset $\mathcal{D}_2(N)$ (not utilized for estimation purposes)

$$\widehat{n}(N) = \arg \min_{n \in [1, N-M+1]} \mathrm{SS}(n) \quad (11)$$

where

$$\mathrm{SS}(n) = \sum_{t=t-M+1}^{N} \sum_{i=1}^{I} \sum_{j=J/2+1}^{J} \left[m_i - \widehat{\boldsymbol{h}}_n^{\mathrm{T}}(N) \boldsymbol{\varphi}_n^{ij}(t) \right]^2 \quad (12)$$

denotes the sum of squared modeling errors.

Unlike information criteria, the cross validation approach does not require any specific assumptions about the nature of modeling errors, except that the sets $\mathcal{D}_1(N)$ and $\mathcal{D}_2(N)$ are two independent samples drawn from the same sample space. The clear advantage of the cross validation approach is that it checks an actual performance of the created model on real data, while the information criteria predict its hypothetical performance on a virtual (i.e., nonexistent) validation data set. The clear disadvantage is that only a portion of the available data is used for parameter estimation purposes.

C. Experimental verification

Our test-stand, depicted in Fig. 4, is an open configuration of the commercial product of the company RADWAG Wagi Elektroniczne (www.radwag.com). The weighing conveyor of length $L = 350\,\mathrm{mm}$ and mass $M = 3.5\,\mathrm{kg}$ is mounted on a C3 accuracy class [21] strain gauge load cell operating in the range 3 kg – 5 kg. This popular industrial force transducer, consisting of four strain gauges connected in a Wheatstone bridge, outputs a differential signal proportional to the applied force. With a 10 V supply, the 2 mV/V electrical sensitivity bridge offers a full-scale differential signal output to be about 20 mV. In the adopted system the bridge output signal was interfaced directly to a specialized 20-bit A/D converter.

Our database consisted of multiple sets of independent measurements obtained for $I = 7$ test loads (metal bars of the same active length $l = 130\,\mathrm{mm}$ – see Fig 1) with 7 different masses ($m_1 = 25\,\mathrm{g}$, $m_2 = 50\,\mathrm{g}$, $m_3 = 100\,\mathrm{g}$, $m_4 = 200\,\mathrm{g}$, $m_5 = 350\,\mathrm{g}$, $m_6 = 500\,\mathrm{g}$, $m_7 = 750\,\mathrm{g}$), under 3 conveyor belt speeds ($v_1 = 0.54\,\mathrm{m/s}$, $v_2 = 0.94\,\mathrm{m/s}$, $v_3 = 1.34\,\mathrm{m/s}$) and 2 sampling rates ($f_1 = 800\,\mathrm{Hz}$, $f_2 = 1600\,\mathrm{Hz}$). In each case dynamic weighing was repeated $J = 240$ times.

To check and compare different variants of model identification, the measurements $\mathcal{Y}^{ij}(N), j = 1, \ldots, 240$ collected for each mass m_i under given operating conditions were divided into 4 subsets, each of which contained 60 sequences of measurements

$$\begin{aligned} \mathcal{Y}_1^i(N) &= \{y^{ij}(t), j = 1, \ldots, 60, t = 1, \ldots, N\} \\ \mathcal{Y}_2^i(N) &= \{y^{ij}(t), j = 61, \ldots, 120, t = 1, \ldots, N\} \\ \mathcal{Y}_3^i(N) &= \{y^{ij}(t), j = 121, \ldots, 180, t = 1, \ldots, N\} \\ \mathcal{Y}_4^i(N) &= \{y^{ij}(t), j = 181, \ldots, 240, t = 1, \ldots, N\}. \end{aligned}$$

Models were evaluated using the method of 4-fold cross validation, which means that validation was repeated 4 times. During each run one of the subsets $\mathcal{Y}_k^i(N)$, $k = 1, \ldots, 4$ was used to check performance of the model obtained using the remaining 3 subsets. In this way, for each mass m_i the set of 240 estimation errors was obtained

$$\mathcal{E}_i = \{\varepsilon_{il}, l = 1, \ldots, 240\}$$

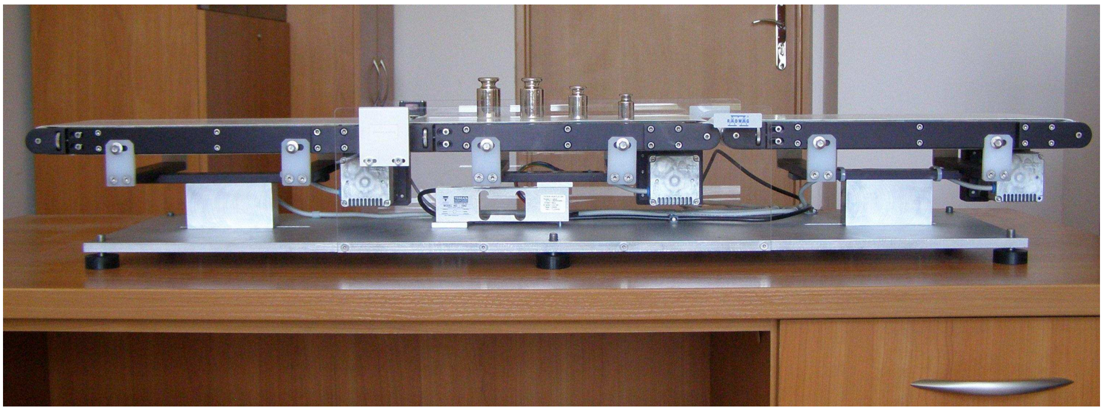

Fig. 4. The experimental test-stand.

where $\varepsilon_{il} = [\widehat{m}_i(N)]_l - m_i$ and $[\widehat{m}_i(N)]_l$ denotes the outcome of the l-th weighing experiment performed for the mass m_i.

The following performance measure was used to quantify the results of weighing

$$\Delta_i = |\widehat{\mu}_i| + 3\widehat{\sigma}_i \tag{13}$$

where $\widehat{\mu}_i$ and $\widehat{\sigma}_i$ denote the population mean and standard deviation, respectively

$$\widehat{\mu}_i = \frac{1}{240}\sum_{l=1}^{240}\varepsilon_{il}, \quad \widehat{\sigma}_i = \sqrt{\frac{1}{239}\sum_{l=1}^{240}(\varepsilon_{il} - \widehat{\mu}_i)^2}.$$

Such a measure combines information about the bias and variance components of the estimation error and has a nice statistical interpretation: under Gaussian assumptions the true weight lies within three standard deviations of its mean with a high probability, namely

$$P(\mu_i - 3\sigma_i \leq \varepsilon_i \leq \mu_i + 3\sigma_i) = 0.997 \tag{14}$$

where $\varepsilon_i = \widehat{m}_i(N) - m_i$ denotes the estimation error. Consequently it holds that

$$P(|\varepsilon_i| > \Delta_i) \cong P(|\varepsilon_i| > |\mu_i| + 3\sigma_i) < 0.003 \tag{15}$$

Based on (13), one can also define a relative performance index

$$\delta_i = \frac{\Delta_i}{m_i} 100[\%] \tag{16}$$

Note that, according to (15), the probability that the relative error $|\varepsilon_i|/m_i$ exceeds δ_i is smaller than 0.003.

Fig. 5 shows the results of comparison of three approaches to model order selection (AIC, BIC, CV) obtained for 3 test loads ($m_1 = 25\,\mathrm{g}$, $m_5 = 350\,\mathrm{g}$, $m_7 = 750\,\mathrm{g}$), 3 conveyor belt speeds ($v_1 = 0.54\,\mathrm{m/s}$, $v_2 = 0.94\,\mathrm{m/s}$, $v_3 = 1.34\,\mathrm{m/s}$) and 2 sampling rates ($f_1 = 800\,\mathrm{Hz}$, $f_2 = 1600\,\mathrm{Hz}$). The following order-adaptive version of (4) was used to asses the item's weight

$$\widehat{m}(N) = \widehat{\boldsymbol{h}}^{\mathrm{T}}_{\widehat{n}(N)}(N)\boldsymbol{\psi}_{\widehat{n}(N)}(N) \tag{17}$$

where $\widehat{n}(N)$ denotes the order selected according to AIC, BIC or CV[1].

In 15 out of 18 cases model order selection based on the information criteria (AIC, BIC) yielded better results than selection based on the cross-validatory analysis, which can be explained by the fact that in the second case only half of the available test data was used for the purpose of parameter estimation. This effect is more pronounced when the sampling rate (i.e., data size) is small - for the higher sampling rate the differences between the compared approaches are small. In 9 cases the AIC criterion yielded better results (often marginally better) than the BIC criterion, while the opposite was true in 2 cases only. In the remaining 7 cases both criteria yielded the same results (after rounding). Based on this evidence, in all further tests model orders were selected using the AIC criterion.

As expected, the estimation accuracy increases with growing sampling frequency. Note, however, that there is no clear relationship between the estimation accuracy and the conveyor belt speed – the lower speed (which results in a larger number of measurements) does not necessarily guarantee the higher weighing precision – cf. Figs. 5a-5f. Similarly, although the absolute errors can be expected to increase with the mass of the weighed object, this is not always the case. One of the possible explanations of these anomalies is that some combinations of the mass and speed cause excitation of the internal resonant modes of the weighing system, which results in larger (locally) measurement errors.

Denote by $N_1 = t_2 - t_1 + 1$ the length of the initial transient weighing phase (during which the item gradually slides onto the weighing platform) and by $N_2 = t_3 - t_2$ – the length of the full-load phase (during which the entire item remains on the platform). Information about N_1, N_2 and the total number of measurements available under different operating conditions is presented in Tab I.

Typical values of the model order selected by the compared methods under different operating conditions are shown in Tab. II. Unlike initially expected, the typical values of $\widehat{n}(N)$ exceed N_2 and are pretty close to N, which means that the

[1]Note that in the latter case the method of cross validation was used twice: first as a tool for model order selection, and then as a method for objective evaluation of the results of modeling.

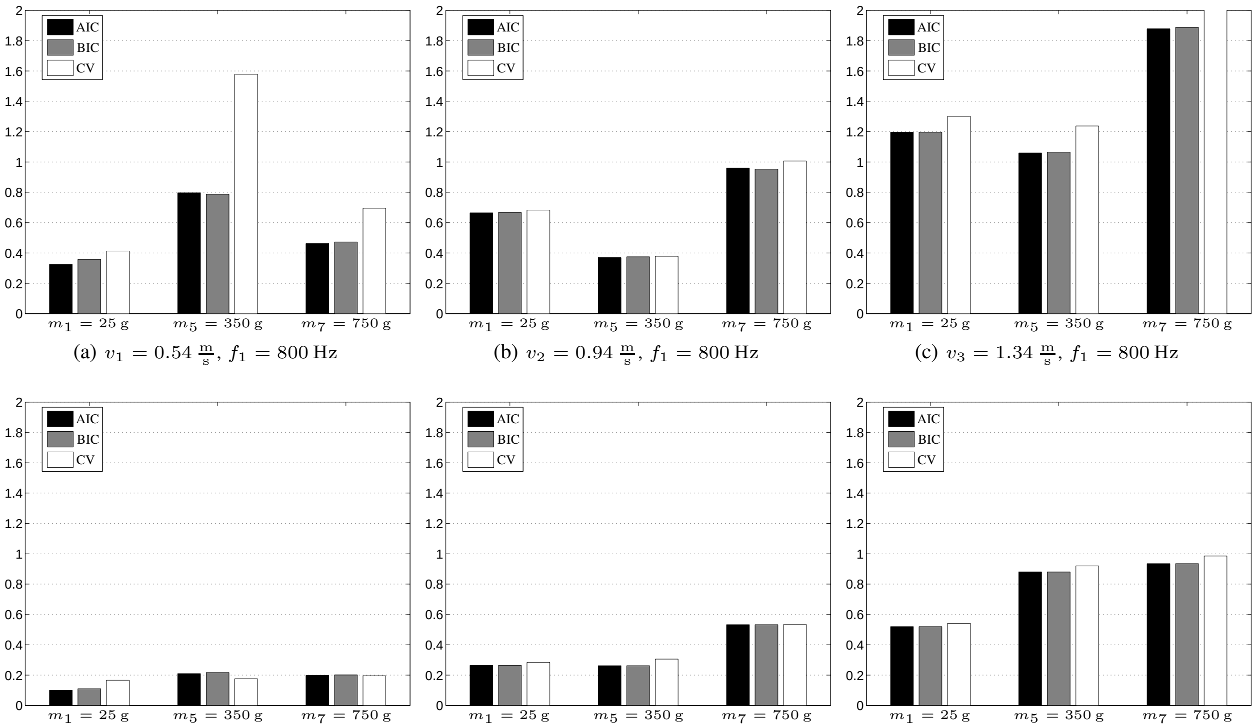

(a) $v_1 = 0.54\,\frac{\mathrm{m}}{\mathrm{s}}$, $f_1 = 800\,\mathrm{Hz}$
(b) $v_2 = 0.94\,\frac{\mathrm{m}}{\mathrm{s}}$, $f_1 = 800\,\mathrm{Hz}$
(c) $v_3 = 1.34\,\frac{\mathrm{m}}{\mathrm{s}}$, $f_1 = 800\,\mathrm{Hz}$

(d) $v_1 = 0.54\,\frac{\mathrm{m}}{\mathrm{s}}$, $f_2 = 1600\,\mathrm{Hz}$
(e) $v_2 = 0.94\,\frac{\mathrm{m}}{\mathrm{s}}$, $f_2 = 1600\,\mathrm{Hz}$
(f) $v_3 = 1.34\,\frac{\mathrm{m}}{\mathrm{s}}$, $f_2 = 1600\,\mathrm{Hz}$

Fig. 5. The values of the performance measure $\Delta_i = |\widehat{\mu}_i| + 3\widehat{\sigma}_i$ obtained using the method of 4-fold cross validation, for the global FIR model of the dynamic weighing system. Model order is selected using the Akaike information criterion (AIC), the Bayesian information criterion (BIC) or the crossvalidatory analysis (CV)

TABLE I
THE LENGTH OF THE INITIAL TRANSIENT WEIGHING PHASE N_1, FULL-LOAD PHASE N_2 AND THE TOTAL NUMBER OF MEASUREMENTS $N = N_1 + N_2$ AVAILABLE UNDER DIFFERENT WEIGHING CONDITIONS.

	$f_1 = 800$ Hz			$f_1 = 1600$ Hz		
v	N_1	N_2	N	N_1	N_2	N
$v_1 = 0.54$ [m/s]	194	326	520	388	652	1040
$v_2 = 0.94$ [m/s]	113	187	300	226	374	600
$v_3 = 1.34$ [m/s]	79	131	210	158	262	420

TABLE II
MODEL ORDER SELECTED BY AIC, BIC. AND CV UNDER DIFFERENT WEIGHING CONDITIONS.

	$f_1 = 800$ Hz			$f_1 = 1600$ Hz		
v	AIC	BIC	CV	AIC	BIC	CV
$v_1 = 0.54$ [m/s]	502	452	282	1013	1011	500
$v_2 = 0.94$ [m/s]	282	265	282	582	582	582
$v_3 = 1.34$ [m/s]	190	189	192	402	402	402

data collected in the initial transient phase of weighing pay an important role in weight estimation.

IV. MODEL DEBIASING

Fig. 6a shows the results of the 4-fold cross validation of the global model obtained, for $v_2 = 0.94\,\mathrm{m/s}$, $f_1 = 800\,\mathrm{Hz}$ and all 7 test loads (in the way described earlier, with AIC-based order selection). Fig 6b provides information about the mean value μ_i and standard deviation σ_i of estimation errors observed for different values of m_i. It can be seen that the estimator $\widehat{m}(N)$ is biased in the range of small values of the mass. Since for $m_i < 350\,\mathrm{g}$ the bias constitutes a significant contribution to the overall performance index Δ_i, a simple debiasing technique was designed and experimentally verified. The bias can be evaluated for each test load using the formula

$$\widehat{c}_i(N) = \frac{1}{J}\sum_{j=1}^{J} \widehat{\boldsymbol{h}}^{\mathrm{T}}_{\widehat{n}(N)}(N)\boldsymbol{\varphi}^{ij}_{\widehat{n}(N)}(N) - m_i. \qquad (18)$$

The debiasing procedure depends on the operating mode of the checkweigher. In the restricted load mode, the desired (nominal) weight of the item, say m_i, is known prior to weighing. The checkweigher is used only to eliminate items that are too heavy or too light – their actual weight, as long as it differs much from m_i is usually less important. The restricted mode is usually applied in situations where the price of the merchandise is fixed and the amount can be precisely dozed (e.g. packages containing loose materials). In such a case the debiased load estimate can be obtained using the following simple formula

$$\widetilde{m}_i(N) = \widehat{m}(N) - \widehat{c}_i(N). \qquad (19)$$

When the weight of the goods/packages cannot be precisely controlled (as it takes place for fruits, vegetables, portions of meat etc.) and the price depends on the weight, the checkweigher is operated in the unrestricted load mode. In this case we know only that the true weight remains within a certain range of values, e.g. $m \in [m_1, m_I]$, and its accurate

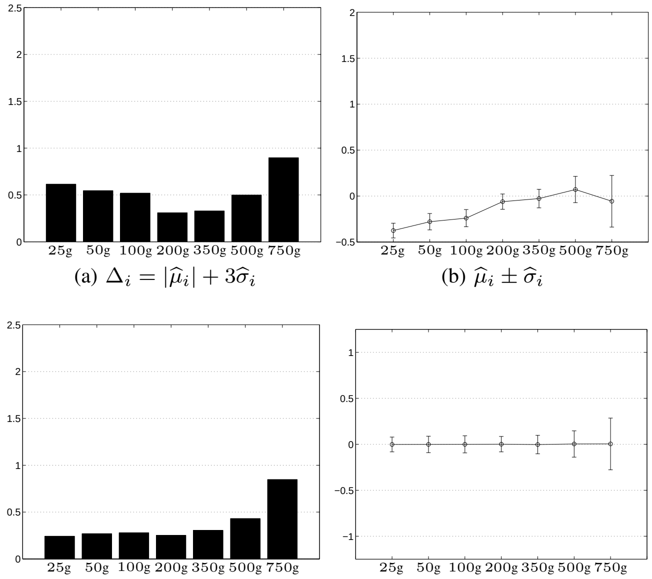

(a) $\Delta_i = |\widehat{\mu}_i| + 3\widehat{\sigma}_i$ (b) $\widehat{\mu}_i \pm \widehat{\sigma}_i$

(c) $\Delta_i = |\widehat{\mu}_i| + 3\widehat{\sigma}_i$ (d) $\widehat{\mu}_i \pm \widehat{\sigma}_i$

Fig. 6. Results of the 4-fold cross validation of the global model (a) and its debiased version (c). The remaining two plots show the estimation bias μ_i and standard deviation σ_i (vertical bars) observed for the global model (b) and for debiased global model (d).

measurement is needed for correct product pricing and/or labeling. When weighing is performed in the unrestricted load mode, the necessary bias correction can be worked out using a piecewise linear interpolation: $\widehat{c}(N) = \widehat{c}_1(N)$ if $\widehat{m}(N) < m_1$, $\widehat{c}(N) = \widehat{c}_I(N)$ if $\widehat{m}(N) \geq m_I$ and

$$\widehat{c}(N) = \widehat{c}_i(N) + \frac{\widehat{m}(N) - m_i}{m_{i+1} - m_i}[\widehat{c}_{i+1}(N) - \widehat{c}_i(N)] \tag{20}$$

if $m_i \leq \widehat{m}(N) < m_{i+1}$. Alternatively, the correction can be based on nonlinear approximation

$$\widehat{c}(N) = g[\widehat{m}(N), \boldsymbol{\alpha}_0] \tag{21}$$

where

$$\boldsymbol{\alpha}_0 = \arg\min_{\boldsymbol{\alpha}} \sum_{i=1}^{I} \{g[m_i, \boldsymbol{\alpha}] - \widehat{c}_i(N)\}^2 \tag{22}$$

and $g[m, \boldsymbol{\alpha}]$ is a nonlinear function of the load m with a certain number of adjustable parameters $\boldsymbol{\alpha} = [a_1, \ldots, a_k]^{\mathrm{T}}$. For example, one can set

$$g[m, \boldsymbol{\alpha}] = a_1 + a_2 m + \ldots + a_k m^{k-1}.$$

The bias-corrected estimate takes the form

$$\widetilde{m}(N) = \widehat{m}(N) - \widehat{c}(N). \tag{23}$$

Figures 6c-6d show the results obtained for the debiased estimator (19). Again, the 4-fold cross validation was applied, which means that the effects of debiasing were verified on a different set of measurements than that used for model identification. Note accuracy improvements in the range of small mass values.

V. Weight estimation based on local modeling

The global model was designed to provide good fit for the entire range of loads – in the case considered from 25 g to 750 g. In practice it often happens that the checkweigher is used to verify the weight of only one type of products with a specified nominal (desired) mass, say m_i. Denote by $\mathcal{D}^i(N) = \{\mathcal{Y}^{ij}(N), j = 1, \ldots, J\}$ the set of measurements collected for the load m_i. An obvious question is whether the local model, i.e., the one based exclusively on the set $\mathcal{D}^i(N)$, can provide more accurate load estimates around m_i than the global model based on the set $\mathcal{D}(N) = \{\mathcal{D}^i(N), i = 1, \ldots, I\}$, described in the previous section.

Parameters of the local model can be estimated using the formula

$$\begin{aligned}\widehat{\boldsymbol{h}}_n^i(N) &= \arg\min_{\boldsymbol{h}_n} \sum_{t=N-M+1}^{N} \sum_{j=1}^{J} [m_i - \boldsymbol{h}_n^{\mathrm{T}} \boldsymbol{\varphi}_n^{ij}(t)]^2 \\ &= \left[\sum_{t=N-M+1}^{N} \sum_{j=1}^{J} \boldsymbol{\varphi}_n^{ij}(t) [\boldsymbol{\varphi}_n^{ij}(t)]^{\mathrm{T}} \right]^{-1} \\ &\quad \times \left[\sum_{t=N-M+1}^{N} \sum_{j=1}^{J} \boldsymbol{\varphi}_n^{ij}(t) m_i \right]\end{aligned} \tag{24}$$

and the order n can be selected by means of minimizing the AIC statistic

$$\widehat{n}_i(N) = \arg\min_n \mathrm{AIC}_i(n) \tag{25}$$

where

$$\mathrm{AIC}_i(n) = K_i \log \mathrm{RSS}_i(n) + 2n, \tag{26}$$

$K_i = JM$ and $\mathrm{RSS}_i(n)$ denotes the residual sum of squares

$$\mathrm{RSS}_i(n) = \sum_{t=t-M+1}^{N} \sum_{j=1}^{J} \Big[m_i - [\widehat{\boldsymbol{h}}_n^i(N)]^{\mathrm{T}} \boldsymbol{\varphi}_n^{ij}(t) \Big]^2. \tag{27}$$

The final weight estimates based on the local model tuned in to the load m_i has the form

$$\widehat{m}_i(N) = [\widehat{\boldsymbol{h}}^i_{\widehat{n}_i(N)}(N)]^{\mathrm{T}} \boldsymbol{\psi}_{\widehat{n}_i(N)}(t). \tag{28}$$

Table III presents results – absolute performance measures $\Delta_i = |\widehat{\mu}_i| + 3\widehat{\sigma}_i$ and relative performance measures $\delta_i = \Delta_i / n_i$, evaluated via 4-fold cross validation – observed when the local model tuned in to the load $m_i, i = 1, \ldots, 7$ is used to estimate the load $m_k, k = 1, \ldots, 7$. As expected, the best performance is achieved when $m_k = m_i$ and it gradually deteriorates as the difference $|m_k - m_i|$ becomes larger. Importantly, when $m_k = m_i$, local models outperform the debiased global model, i.e., they yield noticeably more accurate load estimates.

The results obtained for the local model tuned in to the load $m_4 = 200$ g are shown in Fig. 7. Similarly as in the case of the global model, the performance of the local model is limited mainly by bias errors which occur when $m_k \neq m_i$. To remove bias, one can use the technique described in the previous section. Note that the results yielded by the debiased local model [Fig. 7c] are better than the analogous results yielded by the debiased global model [Fig. 6c].

TABLE III
ABSOLUTE PERFORMANCE MEASURE ($\Delta_i = |\widehat{\mu}_i| + 3\widehat{\sigma}_i$ – UPPER TABLE) AND RELATIVE PERFORMANCE MEASURE ($\delta_i = \Delta_i/m_i$ – LOWER TABLE), EVALUATED VIA 4-FOLD CROSS VALIDATION, OBSERVED WHEN THE LOCAL MODEL TUNED IN TO THE LOAD $m_i, i = 1, \ldots, 7$ (HORIZONTAL AXIS) IS USED TO ESTIMATE THE LOAD $m_k, k = 1, \ldots, 7$ (VERTICAL AXIS).

k	25g	50g	100g	200g	350g	500g	750g
1	0.13g	0.67g	1.71g	3.62g	6.75g	9.80g	13.0g
2	0.40g	0.18g	0.59g	1.52g	2.95g	4.41g	7.20g
3	0.51g	0.41g	0.11g	0.58g	1.27g	2.14g	3.79g
4	0.57g	0.50g	0.32g	0.14g	0.48g	1.04g	2.29g
5	0.59g	0.55g	0.43g	0.30g	0.20g	0.59g	1.34g
6	0.60g	0.60g	0.51g	0.44g	0.42g	0.36g	0.93g
7	0.68g	0.63g	0.57g	0.56g	0.63g	0.65g	0.59g

(a)

k	25g	50g	100g	200g	350g	500g	750g
1	0.52%	1.34%	1.71%	1.81%	1.93%	1.96%	1.73%
2	1.60%	0.35%	0.59%	0.76%	0.84%	0.88%	0.96%
3	2.04%	0.82%	0.11%	0.29%	0.36%	0.43%	0.51%
4	2.27%	1.00%	0.32%	0.07%	0.14%	0.21%	0.30%
5	2.37%	1.10%	0.43%	0.15%	0.06%	0.12%	0.18%
6	2.40%	1.20%	0.51%	0.22%	0.12%	0.07%	0.12%
7	2.71%	1.26%	0.57%	0.28%	0.18%	0.13%	0.08%

(b)

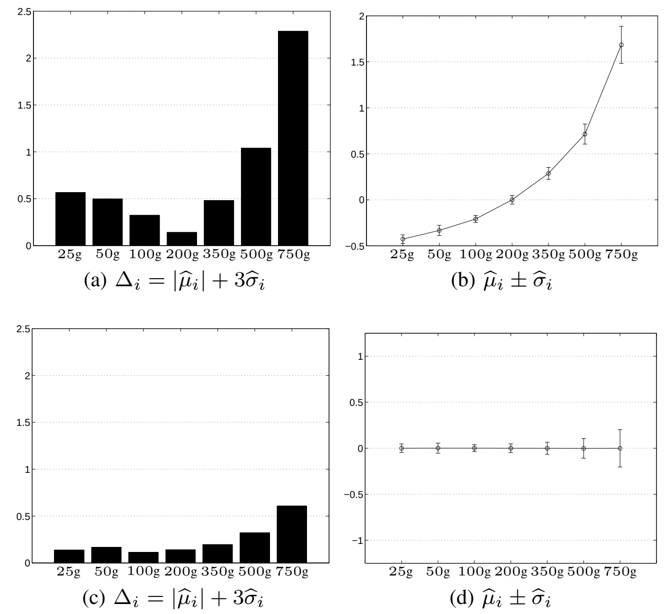

(a) $\Delta_i = |\widehat{\mu}_i| + 3\widehat{\sigma}_i$ (b) $\widehat{\mu}_i \pm \widehat{\sigma}_i$

(c) $\Delta_i = |\widehat{\mu}_i| + 3\widehat{\sigma}_i$ (d) $\widehat{\mu}_i \pm \widehat{\sigma}_i$

Fig. 7. Results of the 4-fold cross validation of the local model tuned in to the load $m_4 = 200$ g (a) and its debiased version (c). The remaining two plots show the estimation bias μ_i and standard deviation σ_i (vertical bars) observed for the local model (b) and for debiased local model (d).

TABLE IV
ABSOLUTE PERFORMANCE MEASURE ($\Delta_i = |\widehat{\mu}_i| + 3\widehat{\sigma}_i$ – UPPER TABLE) AND RELATIVE PERFORMANCE MEASURE ($\delta_i = \Delta_i/m_i$ – LOWER TABLE), EVALUATED VIA 4-FOLD CROSS VALIDATION, OBSERVED WHEN THE DEBIASED LOCAL MODEL TUNED IN TO THE LOAD $m_i, i = 1, \ldots, 7$ (HORIZONTAL AXIS) IS USED TO ESTIMATE THE LOAD $m_k, k = 1, \ldots, 7$ (VERTICAL AXIS).

k	25g	50g	100g	200g	350g	500g	750g
1	0.13g	0.16g	0.14g	0.21g	0.33g	0.56g	0.96g
2	0.14g	0.17g	0.12g	0.18g	0.24g	0.48g	0.86g
3	0.13g	0.18g	0.11g	0.15g	0.24g	0.40g	0.66g
4	0.14g	0.17g	0.11g	0.14g	0.20g	0.32g	0.61g
5	0.15g	0.16g	0.12g	0.14g	0.20g	0.36g	0.53g
6	0.15g	0.18g	0.14g	0.16g	0.20g	0.35g	0.47g
7	0.23g	0.23g	0.22g	0.21g	0.28g	0.36g	0.57g

(a)

k	25g	50g	100g	200g	350g	500g	750g
1	0.52%	0.33%	0.14%	0.10%	0.09%	0.11%	0.13%
2	0.54%	0.35%	0.12%	0.09%	0.07%	0.10%	0.11%
3	0.54%	0.35%	0.11%	0.08%	0.07%	0.08%	0.09%
4	0.56%	0.33%	0.11%	0.07%	0.06%	0.06%	0.08%
5	0.60%	0.33%	0.12%	0.07%	0.06%	0.07%	0.07%
6	0.61%	0.37%	0.14%	0.08%	0.06%	0.07%	0.06%
7	0.93%	0.46%	0.22%	0.11%	0.08%	0.07%	0.08%

(b)

Table IV shows results obtained for debiased local models tuned in to different loads. The accuracy improvements achieved via debiasing are evident. On the average the best results are obtained for debiased local models tuned in to loads placed in the middle of the considered measurement range: $m_i \cong (m_1 + m_I)/2$.

Finally, Fig. 8 presents 3-D visualization of the results shown in tables III (obtained for local models prior to debiasing) and IV (obtained for local models after debiasing) – note the vertical scale differences between Fig. 8(a) and Fig. 8(d), and between Fig. 8(b) and Fig. 8(e), respectively.

The drawback of the debiasing procedure, originally developed for the global model, is the large number of test measurements that must be taken for each test load $m_i, i = 1, \ldots, 7$. For example, the results shown in Table IV and Figs. 8b, 8e were obtained for local models created using 7 sets of 180 measurement sequences (the remaining 7 sets of 60 measurement sequences were used for validation purposes) – for each load m_i one set was used to identify the local model tuned in to m_i, and the remaining sets were used to estimate bias coefficients for other loads $m_k \neq m_i$. A natural question arises whether such a large number of measurements is really necessary to obtain a reliable approximation of the debiasing curve. The two rightmost plots in Figure 8 show comparison of the results yielded by the debiased local models in the case where the bias curve is approximated using 180 measurement sequences per each test load [Fig. 8c is just another view of the 3-D bar plot shown in 8b] and in the case where only 10 (randomly selected) measurement sequences per each load are used for the same purpose [Fig.

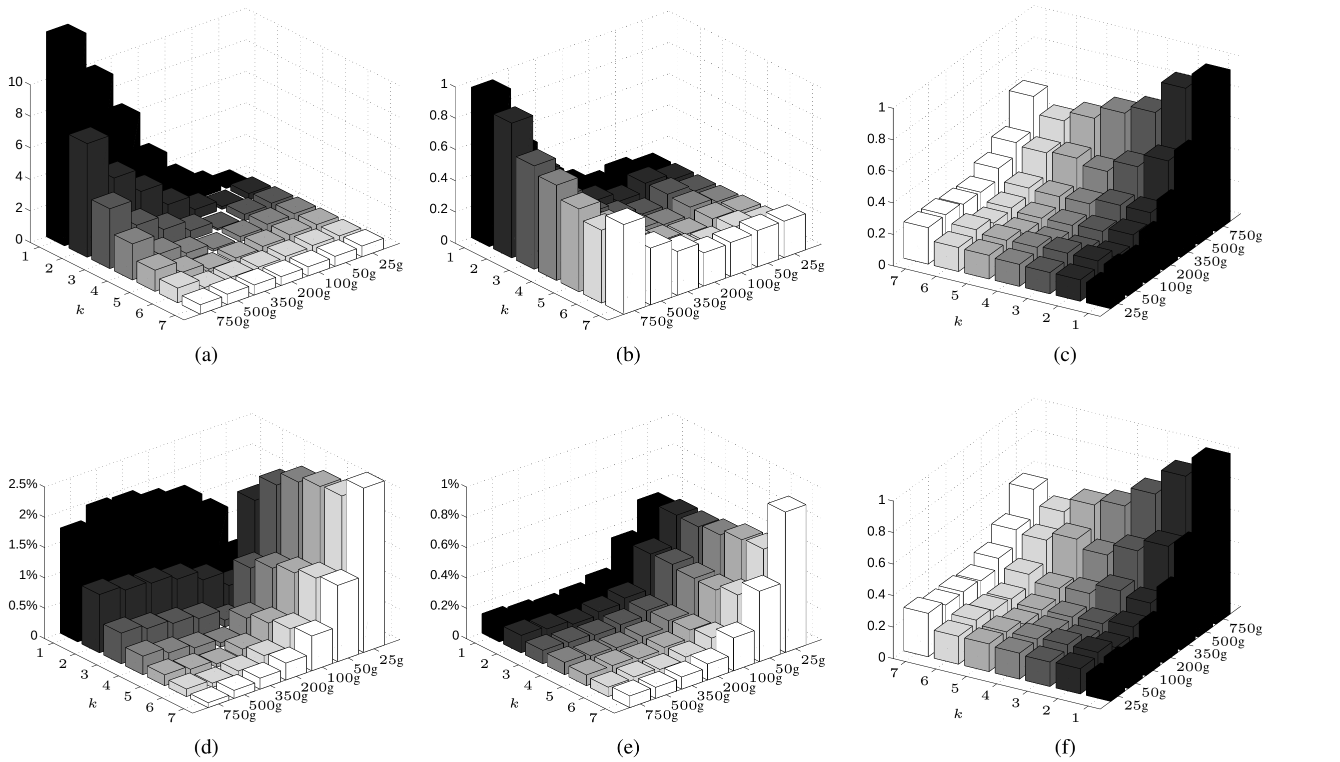

Fig. 8. Absolute [$\Delta_i = |\widehat{\mu}_i| + 3\widehat{\sigma}_i$ – plots (a) and (b)] and relative [$\delta_i = \Delta_i/n_i$ – plots (d) and (e)] performance measures, evaluated via 4-fold cross validation, obtained for the local models tuned in to the load m_k [plots (a) and (d)] and debiased local models tuned in to the load m_k [plots (b) and (e)]. The two rightmost plots [(c) and (f)] present the values of the absolute performance measure obtained for the debiased local models when the bias curve is approximated based on 180 training sequences per load, and 10 training sequences per load [plots (c) and (f), respectively]. Note that the plots (b) and (c) visualize the same data.

8f]. Since differences between the two plots are negligible, the simplified debiasing procedure, based on a small number of additional measurements taken for the loads other than m_i, can be applied without deteriorating the weighing accuracy. This also means that the cost of recalibration of the dynamic weighing system (periodic recalibration is recommended by metrological standards) is relatively low.

All conclusions drawn in this section, based on the results obtained under one operating condition ($v_2 = 0.94\,\mathrm{m/s}$, $f_1 = 800\,\mathrm{Hz}$), extend to other operating conditions – the corresponding evidence is not shown because of the lack of space. Therefore, the recommended procedure for tuning the dynamic weighing system can be summarized as follows:

1) Select the conveyor belt speed v and sampling frequency f.
2) Choose the load m_i so that it holds $m_i \cong (m_1+m_I)/2$.
3) Collect $J \geq 100$ measurement sequences for the load m_i: $\mathcal{D}^i(N) = \{y^{ij}(1), \ldots, y^{ij}(N),\ j = 1, \ldots, J\}$.
4) Based on the measurements $\mathcal{D}^i(N)$ identify the best local FIR model: use the method of least squares to estimate model coefficients and the Akaike information criterion to select the most appropriate model order.
5) Collect a small number of additional measurement sequences (e.g. 10) for each test load m_k that differs from the load m_i.
6) Use additional measurements to estimate the the corresponding bias coefficients.

When the checkweigher is operated in the restricted load mode, the steps 5 and 6 need to be taken only when the nominal load changes, i.e., when a new product with nominal mass $m_k \neq m_i$ enters the line. In this case additional measurements should be collected for the new load only.

VI. Comparison with the state-of-the art solutions

The FIR-model based approach to dynamic weighing proposed in this paper will be compared with two state-of-the-art model-free approaches: the subspace identification method proposed in [17], and the time-variant filtering approach described in [15] (which provides similar accuracy as the model-based approach presented in [10]). Figure 9 shows results yielded by the subspace identification method (A), the time-variant filtering approach (B) and four variants of FIR filtering based on: the global model (C), the debiased global model (D), the debiased local model tuned in to the load $m_5 = 350$ g (E), and debiased local models tuned in to each test load $m_i, i = 1, \ldots, 7$ (F). As before, the conveyor belt speed was equal to $v_2 = 0.94\,\mathrm{m/s}$ and the sampling frequency was equal to $f_1 = 800\,\mathrm{Hz}$.

Note that the best results were obtained using the local modeling approach – the debiased local model tuned in to the load m_5 yielded the best results in two cases (m_2, m_7)

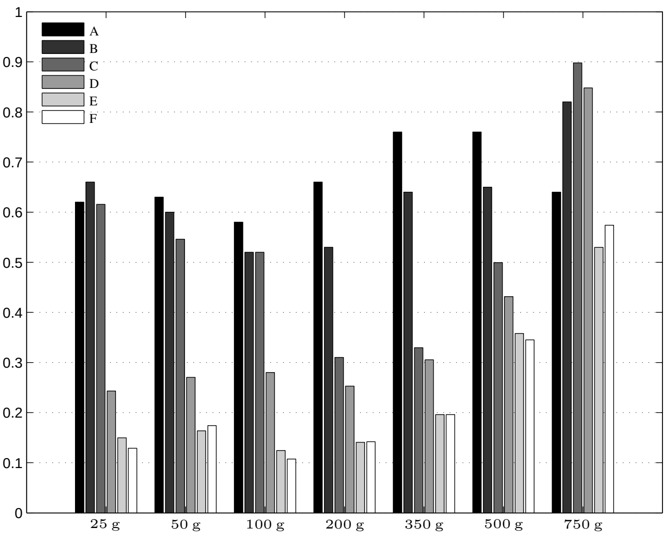

Fig. 9. The values of the absolute performance measure $\Delta_i = |\widehat{\mu}_i| + 3\widehat{\sigma}_i$, evaluated via 4-fold cross validation, obtained using the method of: subspace identification (A), time-variant filtering (B), FIR filtering based on the global model (C), FIR filtering based on the debiased global model (D), FIR filtering based on the debiased local model tuned in to the load $m_5 = 350$ g (E), and FIR filtering based on debiased local models tuned in to each test load $m_i, i = 1, \ldots, 7$ (F).

and the selectively tuned local models – in the remaining four cases (m_1, m_3, m_4, m_5). In the case of the load m_5 both approaches coincide. Since in all cases the performance observed for the two variants of local modeling is very similar, the computationally simpler approach (one model for all loads) is recommended.

Compared with the time-variant filtering approach the local modeling approach offers significant accuracy improvements – the ratio $\Delta_i^{\mathrm{B}}/\Delta_i^{\mathrm{D}}$ ranges from 1.54 for i=7 (750 g) to 4.34 for $i = 1$ (25 g). The debiased global modeling approach is approximately 50% less effective than its local counterpart.

VII. Closing remarks

In the most general formulation the problem of dynamic mass measurement can be stated as a task of finding the mapping from the set of available data, collected during the entire weighing cycle $[t_1, t_4]$, to the mass of the weighed object. This mapping can be identified or, more adequately, approximated, in a direct or indirect way. Our paper belongs to the first category and, as such, it is not based on any phenomenological model of the dynamic weighing system at hand.

Given a large number of data sets, one could train a neural network to capture the relationship between the measurements and the object's mass. We do something similar but simpler, avoiding the large training set problem - we build a high-order linear approximation of the mapping mentioned above, followed by a simple nonlinear correction step.

There are two likely reasons that make the proposed approach work better than the state-of-the-art methods. First, unlike the indirect, identification-based approaches described in [15] and [17], the new method is capable of using additional data from the initial phase of weighing $[t_1, t_2]$, during which the weighed object gradually slides onto the weighing conveyor. Although the direct, time-variant filtering approach presented in [15] does the same thing (it incorporates measurements from the interval $[t_1, t_3]$), it is less flexible as the applied filter is equipped with a much smaller number of tunable parameters. Second, unlike the existing approaches, the proposed method accounts for some nonlinear features of the dynamic weighing system.

Although the proposed approach was developed for a particular type of a dynamic weighing system – the conveyor belt checkweigher – all design steps, including selection of the number of degrees of freedom (order of the FIR filter), are data-adaptive, and hence they can be easily extended to other devices and setups, such as systems for dynamic weighing of vehicles and trains described in [2] – [5]. Of course, some additional experimental work would be needed to check and validate operation of the FIR-model based scheme under such new circumstances.

VIII. Conclusion

The problem of dynamic weighing using conveyor belt type checkweigher was considered. The proposed solution – the filtering scheme based on the FIR model of the response of the weighing system – guarantees up to four times higher weighing accuracy than the existing state-of-the-art solutions.

References

[1] *International recommendation OIML R 51-1, Automatic catchweighing instruments. Part 1: Metrological and technical requirements - Test*, 2006.

[2] M. Niedźwiecki and A. Wasilewski, "Application of adaptive filtering to dynamic weighing of vehicles," *Control Engineering Practice*, vol. 4, no. 5, pp. 635–644, 1996.

[3] T. Guo, D. Frangopol, and Y. Chen, "Fatigue reliability assessment of steel bridge details integrating weigh-in-motion data and probabilistic finite element analysis," *Computers and Structures*, vol. 112, pp. 245–257, 2012.

[4] M. Niedźwiecki and A. Wasilewski, "New algorithms for dynamic weighing of trains," *Control Engineering Practice*, vol. 5, no. 5, pp. 705–715, 1997.

[5] E. Meli and L. Pugi, "Preliminary development, simulation and validation of a weigh in motion system for railway vehicles," *Meccanica*, vol. 48, no. 10, pp. 2541–2565, 2013.

[6] M. Tariq, W. Balachandran, and S. Song, "Checkweigher modeling using dynamical subsystems," in *Proc. 1995 IEEE Industry Applications Conference*, October 1995, pp. 1715–1721.

[7] M. McGuinness, D. Jenkins, and G. Senaratne, "Modelling the physics of high-speed weighing," Mathematics in Industry Information Service, Tech. Rep., 2005.

[8] G. Boschetti, R. Caracciolo, D. Richiedei, and A. Trevisani, "Model-based dynamic compensation of load cell response in weighing machines affected by environmental vibrations," *Mechanical Systems and Signal Processing*, vol. 34, no. 12, pp. 116–130, 2013.

[9] W.-Q. Shu, "Dynamic weighing under nonzero initial conditions," *IEEE Trans. Instrum. Meas.*, vol. 42, no. 4, pp. 806–811, August 1993.

[10] M. Meller, M. Niedźwiecki, and P. Pietrzak, "Adaptive filtering approach to dynamic weighing: a checkweigher case study," in *Proc. 19th IFAC World Congress*, November 2014, pp. 151–155.

[11] J. Piskorowski, "Some aspects of dynamic reduction of transient duration in delay-equalized Chebyshev filters," *IEEE Trans. Instrum. Meas.*, vol. 57, no. 8, pp. 1718–1724, August 2008.

[12] J. Piskorowski and T. Barciński, "Dynamic compensation of load cell response: A time-varying approach," *Mechanical Systems and Signal Processing*, vol. 22, no. 7, pp. 1694–1704, 2008.

[13] J. Piskorowski and M. de Anda, "A new class of continuous-time delay-compensated parameter-varying low-pass elliptic filters with improved dynamic behavior," *IEEE Trans. Circuits Syst. I, Reg. Papers*, vol. 56, no. 1, pp. 179–189, January 2009.

[14] P. Pietrzak, "Dynamic mass measurement using a discrete time-variant filter," in *Proc. IEEE 26th Convention of Electrical and Electronics Engineers in Israel*, August 2010, pp. 5927–5932.

[15] P. Pietrzak, M. Meller, and M. Niedźwiecki, "Dynamic mass measurement in checkweighers using a discrete time-variant low-pass filter," *Mechanical Systems and Signal Processing*, vol. 48, no. 1-2, pp. 67–76, 2014.

[16] A. Pawlowski, F. Rodríguez, J. Sánchez-Hermosilla, and S. Dormido, "Fast nonstationary filtering for adaptive weighing system," in *Proc. IEEE 20th Conference on Emerging Technologies and Factory Automation*, September 2015, pp. 1–6.

[17] I. Markovsky, "Comparison of adaptive and model-free methods for dynamic measurement," *IEEE Sign. Process. Lett.*, vol. 22, no. 8, pp. 1094–1097, 2015.

[18] H. Akaike, "A new look at the statistical model identification," *IEEE Transactions on Automatic Control*, vol. 19, no. 6, pp. 716–723, 1974.

[19] G. Schwarz, "Estimating the dimension of a model," *Annals of Statistics*, vol. 6, no. 2, pp. 461–464, 1978.

[20] S. Arlot and A. Celisse, "A survey of cross-validation procedures for model selection," *Statistics Surveys*, vol. 4, pp. 40–79, 2010.

[21] *International recommendation OIML R 60, Metrological regulation for load cells*, 2000.